Draft version March 6, 2024
Typeset using LaTeX default style in AASTeX63

arXiv:2003.02290v2 [astro-ph.EP] 14 Aug 2020

Peas in a Pod? Radius correlations in Kepler multi-planet systems

Lena Murchikova [1] and Scott Tremaine [1]

[1] *Institute for Advanced Study*
1 Einstein Drive
Princeton, NJ 08540, USA

ABSTRACT

We address the claim of Weiss et al. (2018) that the radii of adjacent planets in *Kepler* multi-planet systems are correlated. We explore two simple toy models—in the first the radii of the planets are chosen at random from a single universal distribution, and in the second we postulate several types of system with distinct radius distributions. We show that an apparent correlation between the radii of adjacent planets similar to the one reported by Weiss et al. (2018) can arise in both models. In addition the second model fits the radius and signal-to-noise distribution of the observed planets. We also comment on the validity of a commonly used correction that is used to estimate intrinsic planet occurrence rates, based on weighting planets by the inverse of their detectability.

Keywords: planets and satellites: general — planets and satellites: detection — methods: statistical

1. INTRODUCTION

Weiss et al. (2018, hereafter W18) reported correlations in the characteristics of neighbouring planets in multi-planet systems – a phenomenon they called "peas in a pod". One of these correlations is in the planetary radii: as stated by W18, "each planet is more likely to be the size of its neighbor than a size drawn at random from the distribution of observed planet sizes". Here we show that the correlation found by W18 can be largely produced by observational selection effects and/or system-to-system variations in the distribution of planetary radii.

Before beginning it is worthwhile to describe the relevant hypotheses more carefully. There are (at least) three logical possibilities:

(i) "Planets don't know anything". More formally, this hypothesis states that the planet-formation process is universal, in the sense that the probability that a planet has radius in a small range $R_p \to R_p + dR_p$ is a universal function, independent of the properties of the host system or the presence or properties of other planets.

(ii) "Planets know about the system they formed in". This is the hypothesis that the probability distribution of radii in a host system labeled by α is some function $p(R_p|\alpha, \mathrm{Per})$ where Per is the orbital period. Thus the radius distribution depends on the properties of the system and the planet's location in it, but not on the presence of other planets.

(iii) "Planets know about other planets". This is the hypothesis that the probability distribution of radii in an N-planet system is a function $p(R_{p1}, \ldots, R_{pN})$ that cannot be separated into a product $\prod_{j=1}^{N} p(R_{pj})$; in other words the correlation coefficient between the distribution of radii of different planets in the same system is non-zero (e.g., Kipping 2018; Mulders et al. 2018; Sandford et al. 2019; He et al. 2019; Gilbert & Fabrycky 2020).

W18 do not state explicitly whether they are arguing for hypothesis (ii) or (iii). Either hypothesis can generate correlations of the kind they observe – for example, if the radius probability distribution in system α is $p(R|\alpha) = \delta(R - R_\alpha)$ with R_α varying from system to system, then all planets in a given system have the same radius and the

lena@ias.edu, tremaine@ias.edu

correlation coefficient measured by W18 will be unity. The main point of this paper, however, is that the correlations they observe can be produced in some respects by hypothesis (i) and in most respects by a simple version of hypothesis (ii). We stress that we consider only the correlation between the radii of adjacent planets and not the other correlations, some of which are discussed by W18. In particular, the full set of parameters also includes periods. In the simplest cases, e.g., hypotheses (i) and (ii), the period and radius distributions are separable.

The analysis of W18 is based on the "CKS multis" or "CKSM" catalog – a subset of the catalog from the California-Kepler Survey (CKS) containing host stars with more than one detected planet. The CKSM catalog contains 909 planets in 355 multi-planet systems, all with measured signal-to-noise ratio SNR ≥ 10 (see eq. 2). A better procedure would be to work directly with the final (DR25) planet candidate catalog from Kepler and to model the detection efficiency, but since our focus is on the statistical analysis we prefer to use the same sample as W18. An important feature of the CKSM catalog is that it contains only systems with detected planets. Such catalogs are much more difficult to correct for selection effects than catalogs compiled with uniform selection criteria that are independent of whether or not a planet is detected.

Our main arguments concerning hypothesis (i) are contained in Sections 2 and 3. In Section 4 we examine the statistical tests used in this context by Weiss et al. (2018), Millholland et al. (2017), Weiss & Petigura (2019) and others to correct for detection biases. We comment on the intrinsic planet radius distribution and the observed SNR distribution and on correlations between the radii of adjacent large planets in Sections 5 and 6. Section 7 contains our main arguments concerning hypothesis (ii). We summarize in Section 8. The goal of this work is not to provide a state-of-the-art model for the observed data, but rather to discuss the methods that are used to analyze such data.

2. "PLANETS DON'T KNOW ANYTHING". CREATING MOCK CKS SYSTEMS, DETECTABILITY CRITERIA, AND CORRELATION MEASURES

We create a mock universe in which planets in a given multi-planet system are not correlated in radius. In particular, we make the strong assumption that the distribution of planets in radius in the mock universe is independent of the properties of the stars, the environment, the orbital period, and the properties of the neighboring planets, that is, the probability that a given planet has radius in the range $R_p \to R_p + dR_p$ is a universal function $p(R_p)dR_p$.

For simplicity we postulate that in our mock universe the universal distribution of radii is a power law,

$$p(R_p)dR_p \sim R_p^{-\gamma} dR_p \tag{1}$$

between $R_{\rm min}$ and $R_{\rm max}$. We set $R_{\rm min}$ and $R_{\rm max}$ to be the smallest and largest planet radii observed in the CKSM sample, $0.34\,R_\oplus$ and $13.11\,R_\oplus$. For the power-law exponent we choose $\gamma = 4$. The resulting radius distribution is unrealistic in several respects—it does not produce the gap in the radius distribution centered on $2R_\oplus$ that is observed at short orbital periods, and it produces too many small planets compared to the number of large ones—but it provides a good illustration of the effects of observational selection on correlations. We discuss the reasons for the choice of this model in Section 5. This distribution of planets is the "intrinsic mock" distribution.

The CKSM catalog contains 909 planets. Each planet is characterized by a radius R_{pj}, an orbital period ${\rm Per}_j$, and a host star ($\star_j$) with properties such as radius $R_{\star j}$ and mass $M_{\star j}$ that help to determine the detectability of the planet. We call the combination of host star and orbital period the "position" of planet j. In our mock universe we will randomize the radius of the planet according to various prescriptions but will keep the set of positions fixed, i.e., the same as in the CKSM catalog (other choices of how to randomize are possible; see footnote 3).

In order to populate the CKSM systems we create a uniformly spaced array of 5000 planetary radii R_{pj} between $R_{\rm min}$ and $R_{\rm max}$. Each radius in the array is assigned a weight (w_j) such that $w_j = R_{pj}^{-4} / \sum_i R_{pi}^{-4}$. We then sample from this weighted distribution to populate the CKSM positions one by one with planets. For a given position, we keep drawing planets at random until a planet is detectable based on the signal-to-noise ratio (SNR) criterion (Weiss et al. 2018; Millholland et al. 2017; Zhu 2019; Weiss & Petigura 2019):

$${\rm SNR}[\star; {\rm Per}, R_p] = \frac{(R_p/R_\star)^2}{{\rm CDPP}_{\star 6hr}\sqrt{6\,{\rm hr}/T(\star;{\rm Per})}} \sqrt{\frac{3.5\,{\rm yr}}{\rm Per}} \geq 10, \tag{2}$$

with transit duration estimated as

$$T(\star;{\rm Per}) = 13\,{\rm hr}\left(\frac{\rm Per}{1{\rm yr}}\right)^{1/3}\left(\frac{\rho_\star}{\rho_\odot}\right)^{-1/3}. \tag{3}$$

Here $(R_p/R_\star)^2$ is the fraction of the star's area blocked by the planet during transit, (3.5 yr)/Per is the number of transits over the lifetime of the *Kepler* mission, and $\rho_\star$ and $\rho_\odot$ are the mean densities of the star and the Sun respectively. Finally $\mathrm{CDPP}_{\star 6hr}\sqrt{6\,\mathrm{hr}/T}$ is a measure of the detectability of the planet over the duration of the transit (Christiansen et al. 2012), in which $\mathrm{CDPP}_{\star 6hr}$ (Combined Differential Photon Precision) is a measure of the photometric noise of the star tabulated in units of parts per million (ppm). For a star with $\mathrm{CDPP}_{\star 6hr} = 10$ ppm a 6-hour transit of depth 10 ppm would have SNR = 1 (assuming a box-shaped transit, no gaps in the data, etc.; future studies can and should use a more careful detection model). The sample of planets produced in this way is the "observed mock" sample.

Following W18, we estimated the strength of the apparent correlation between adjacent planetary radii using the Pearson correlation coefficient r in $\log R_p$, as calculated with the package `scipy.stats.pearsonr`. Pearson's r measures a linear relationship between two datasets. The values of r are between -1 and $+1$ with 0 implying no correlation and ± 1 implying an exact linear relationship. The significance level or p-value of Pearson's r depends on the underlying distribution of planetary radii unless the number of points N is sufficiently large (typically $N \gtrsim 500$). Since our data set has an N of almost exactly 500[1], the significance levels of Pearson's r may be biased. For this reason, we have also repeated all of our analyses using the Spearman correlation coefficient r_s, which is a non-parametric estimator and thus more robust. Spearman's r_s is calculated with the package `scipy.stats.spearmanr`.

3. MOCK UNIVERSE VERSUS CKS CATALOG

In the figures, we present the plots related to our mock universe adjacent to the ones obtained from the true CKSM planets. The mock data are presented in red and the true data in blue. Figure 1a shows the intrinsic mock distribution of radii, that is, the distribution of the planets in radius as they are created in our mock universe. Figure 1b shows the mean observed mock distribution, i.e., the distribution observed after applying the signal-to-noise cut (2), averaged over 5000 Monte-Carlo realizations. Figure 1d shows the corresponding distribution of radii in the CKSM sample. Apart from the dip in the CKSM distribution at $2R_\oplus$ the two distributions look qualitatively similar. The dip is real, and is even more prominent in the distribution of planets around single stars in the CKS (Fulton et al. 2017) and for planets with planets with periods between 10 and 100 days, but we have not attempted to reproduce it in the present mock catalog, since our focus is on simple models and not on careful modeling of the observed data (a mock catalog that does reproduce the dip is described in Section 7). We discuss the reasons for choosing a power law with exponent $\gamma = 4$ for the intrinsic radius distribution in the mock universe in Section 5.

Figures 1c and 1e contain scatter plots of the radii of adjacent planets in the mock data and real data, analogous to Figure 2 of W18. In preparing these plots, we applied the swapping criterion of W18, i.e., a pair of adjacent planets $(R_{pj}, R_{p,j+1})$ is plotted only if the planets would still be detectable if their positions were swapped, $\mathrm{Per}_j \leftrightarrow \mathrm{Per}_{j+1}$. The observations, in the panel on the right, show a strong correlation, with Pearson and Spearman correlation coefficients $r = 0.65$ and $r_s = 0.57$, and p-values much less than 10^{-5}, a conclusion already reached by W18. However, our mock samples on the left *also* show a strong correlation in the adjacent planet radii – over 5000 Monte-Carlo realizations the mean Pearson $r = 0.56$, the mean Spearman $r_s = 0.59$, and the corresponding median p-values are much less than 10^{-5}.

A possible concern with this model is that it implies that the number of undetected planets in some systems is much larger than the number of detected ones, which may lead to gravitational instability. However, systems of planets on nearly circular, nearly coplanar orbits are typically stable if the separation between planets exceeds about 10 Hill radii (Pu & Wu 2015). For Earth-mass planets the Hill radius $a(M_\oplus/3M_\odot)^{1/3}$ is 0.01 times the semimajor axis a. Thus up to 15 Earth-mass planets could be found between periods of 1 and 10 days without violating this stability constraint. If the radii of these additional planets are smaller than the detection threshold they would be undetected.

We conclude that even if the distribution of planet radii is independent of the properties of the host system and the properties of adjacent planets [hypothesis (i) of the Introduction], observational selection effects can introduce the correlations found in W18. The physical reason for this conclusion was described by Zhu (2019): if the $\mathrm{CDPP}_{\star 6hr}$ or stellar radius $R_\star$ is large, or the transit duration $T(\star;\mathrm{Per})$ is small, then according to equation (2) all planets in a multi-planet system must have large radii to survive the SNR cut in the CKSM catalog. On the other hand if

[1] W18 had $N = 504$ compared to our $N = 508$. We believe that the difference is due to marginal rounding differences.

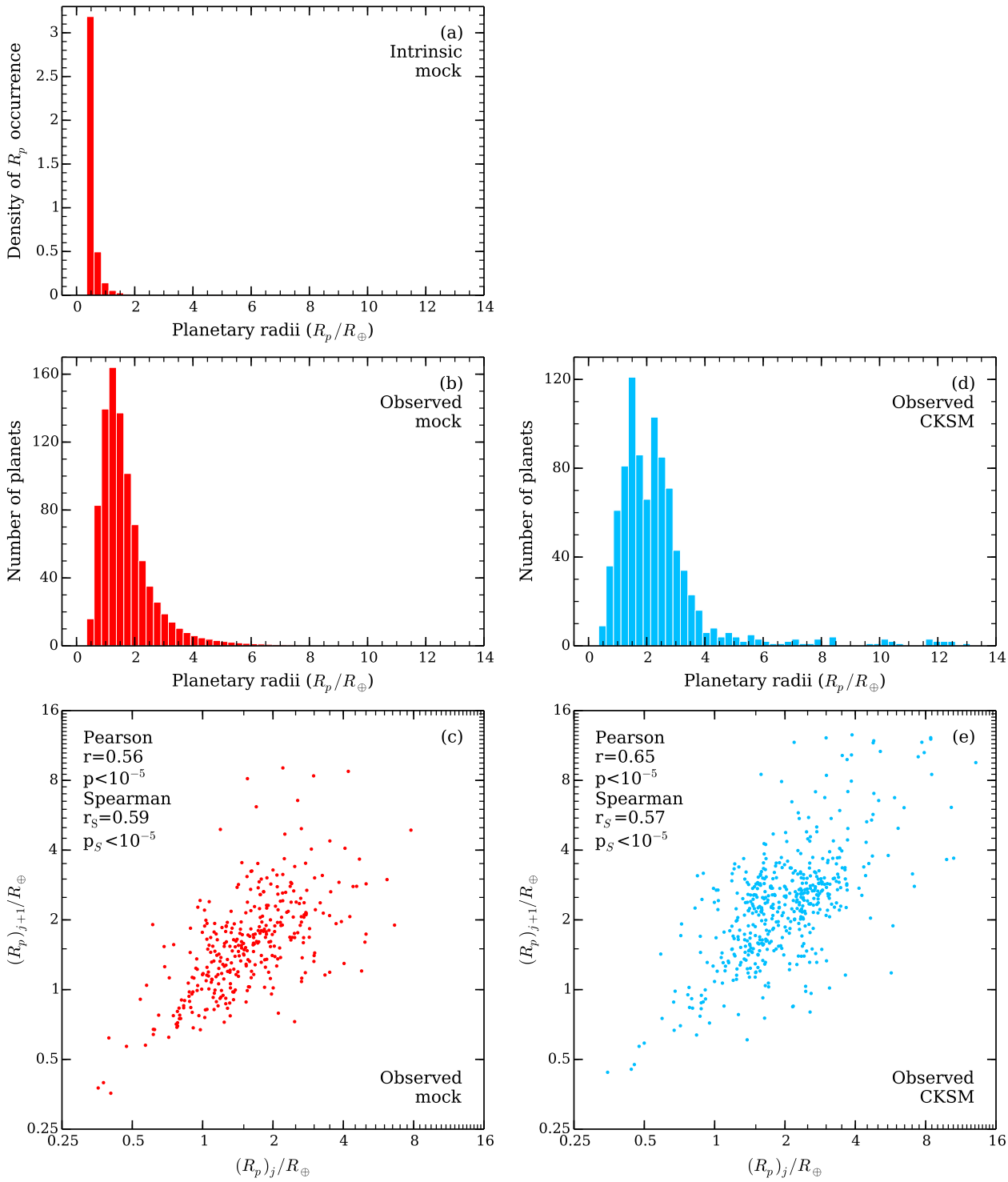


Figure 1. Observations in the mock universe compared to the CKSM sample. Red plots belong to the mock universe and blue to the observed planets. (a) The intrinsic mock distribution of planetary radii. The corresponding CKSM panel is empty, because we do not know the underlying distribution of radii in the real universe. (b) The distribution of radii of the observed mock planets, averaged over 5000 Monte-Carlo realizations. For each of the 909 available $(\star_i, \mathrm{Per}_j)$ positions, we draw a radius at random from the intrinsic mock distribution of radii, apply the SNR cut of equation (2), and repeat until the planet survives the cut. (c) The relation between the radii of adjacent planets R_{pj} and $R_{p,j+1}$ in a typical Monte-Carlo realization of mock planets as described for panel (b). The Pearson/Spearman r and p are averages and medians, respectively, of 5000 Monte-Carlo realizations. (d) and (e) The distribution of radii and the relation between the radii of adjacent planets in the CKSM sample. In panels (c) and (e) we applied the swapping criterion of W18, i.e., a pair of adjacent planets is plotted only if the planets would still be detectable if their positions were swapped.

$\mathrm{CDPP}_{\star 6hr}$ or $R_\star$ is small, or $T(\star;\mathrm{Per})$ is large, then both large and small planets can be detected, but the steep slope of the radius distribution means that most planets in a multi-planet system will be small.

4. BOOTSTRAP AND DETECTABILITY WEIGHTING

To further examine the role of detection biases we repeat the bootstrap simulation in W18. We draw planetary radii at random with replacement from the observed radius distribution, mock or real, to populate the CKS positions, i.e. $\{\star_i, \mathrm{Per}_i\}$, then apply the SNR cut (2). If the planet radius fails the cut, we draw another radius until all 909 available positions in 355 host systems are filled with detectable planets. The result of this approach is shown in Figure 2ad (Figure 2d is directly comparable to W18's Figure 4). In the mock universe we obtain a weak correlation with mean Pearson/Spearman $r = 0.19/0.21$ and median $p \sim 10^{-5}$. In the real universe we obtain Pearson/Spearman $r = 0.09/0.08$ with median $p = 0.11/0.06$. These estimates are based on averaging 5000 Monte-Carlo trials in both the mock and real universes[2].

The failure of this bootstrap test to reproduce the strong correlation between the radii of adjacent planets found in the observed data (Figure 1e) led W18 to conclude that the correlation was likely driven by astrophysics and not observational bias. This conclusion is premature as demonstrated by our mock universe: here the W18 bootstrap test is also unable to reproduce the strong observed correlation, but by construction the correlation is entirely due to observational bias.

The bootstrap test used by W18 is flawed, because drawing the radii at random from the observed distribution gives preference to the most detectable planets over to the most abundant (for example, there are far fewer planets smaller than $1R_\oplus$ in Figure 2d than in Figure 1e). To remedy this flaw, we modified the W18 test by including a weighting procedure. After populating each position $(\star_i, \mathrm{Per}_i)$ with an observable radius R_{pj}, we assign a weight w_j to this radius proportional to the inverse of the number of positions at which it is detectable[3]:

$$w_j = \frac{\tilde{w}_j}{\sum \tilde{w}_k}, \quad \text{where} \quad \tilde{w}_j^{-1} = \sum_i \Theta\left[\mathrm{SNR}(\star_i; \mathrm{Per}_i, R_{pj}) - 10\right], \tag{4}$$

where $\Theta[\cdot]$ is a step function. Then the empirical distribution $p(R_p) = \sum w_j \delta[R_p - R_{pj}]$ should be a more accurate estimate of the intrinsic distribution of radii. This approach is related to a technique known in the statistics literature as balanced bootstrap.

We first compare the distribution of radii derived in this way for the mock universe (Figure 2b) with the intrinsic distribution (Figure 1a). The intrinsic distribution is much steeper than the weighted distribution[4]. We then used these weighted distributions to produce analogs of Figures 1ce, shown in Figures 2cf. We see that the correlations produced in the bootstrap analysis are stronger than in the W18 bootstrap analysis (compare Figure 2cf to 2ac) but still substantially weaker than in the original data, mock or real (Figures 1ce). Averaged over 5000 realizations, balanced bootstrap produces Pearson/Spearman $r = 0.15$ and median $p = 0.001$ in the CKSM data, and Pearson/Spearman $r = 0.33/0.35$ and $p \ll 10^{-5}$ in the mock data, compared to Pearson/Spearman $r \sim 0.6$ in the original data for both the real and the mock universes.

We conclude that neither the W18 bootstrap analysis nor the balanced bootstrap described by equation (4) offers a correct description of the statistics of either the mock or the real data in the CKSM catalog. Informally, bootstrap fails because the data are truncated—planets that lie below some minimum radius are not included in the catalog, and this cutoff varies from star to star.

We can illustrate this problem with a simple example. Consider a population of $N \gg 1$ stars that has two types of planet, one of radius R_1 ("small" planets) and the other of radius $R_2 > R_1$ ("large" planets). The probability that a given star will host a small or large planet is p_1 or p_2, and these two events are independent; we also assume for simplicity that p_1 and p_2 are small enough that the fraction of stars containing more than one planet is negligible.

[2] We stress that the bootstrap algorithm involves somewhat different procedures for the real and mock universes. For the real universe we re-sample the original CKSM data set as there exists only one observational data set. In the mock universe each bootstrap realization is based on independently generating a new set of observed planets.

[3] Other weightings are possible, such as: (i) cycling (R_{pj}, Per_j) pairs through $(\star_i) : \tilde{w}_j^{-1} = \sum_i \Theta[SNR(\star_i; \mathrm{Per}_j, R_{pj}) - 10]$, where i runs over all stars; (ii) Cycling R_{pj} through the shuffled set of Per_k and $(\star_i) : \tilde{w}_j^{-1} = \sum_{i,k} \Theta[SNR(\star_i; \mathrm{Per}_k, R_{pj}) - 10]$, where i runs over all stars and k over all periods; and many others. We present these weightings here to illustrate that the choice of weighting is non-trivial, and should be chosen to be consistent with the rest of the analysis and unambiguously stated.

[4] The following is a heuristic explanation of the problem. The smallest radius in the CKSM catalog is $0.34R_\oplus$, and a planet with this radius would be detectable in 5 of the 909 positions. In contrast, all 59 planets with $R_p > 4.47R_\oplus$ are detectable in all 909 positions (see Figure 5). As a result the detection probability of a planet with $R_p = 0.34R_\oplus$ is only $909/5 = 182$ times smaller than the probability for planets with $R_p > 4.47R_\oplus$. At the same time, in the intrinsic mock distribution the probability of occurrence per unit of log radius of $0.34R_\oplus$ planets is about 2,500 times higher than that of $4.47R_\oplus$ planets.

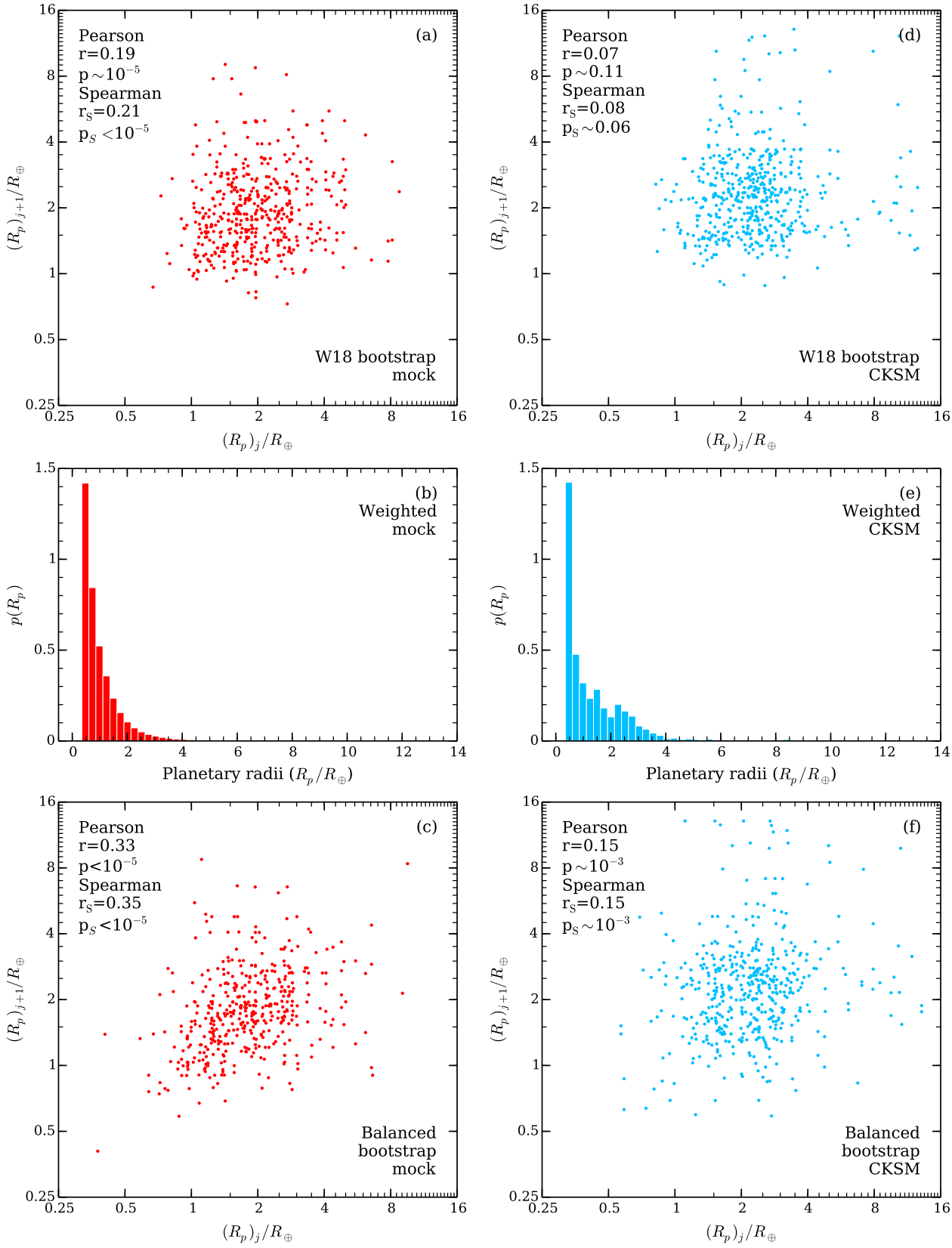


Figure 2. Bootstrap tests. Red plots belong to the mock universe and blue to the observed planets. (a),(d) The results of a typical realization of the bootstrap test in which the planets are drawn from the observed distribution in Figure 1bd; these are directly comparable to the bootstrap tests done by W18. (b),(e) Distribution of planetary radii weighted in detectability according to eq. (4). (c),(f) The results of a typical realization of the balanced bootstrap simulation described in the text. In each scatter plot, the Pearson and Spearman correlation coefficients in $\log R_p$ and their corresponding p-value are printed in the upper left corner and represent the averages and medians of 5000 corresponding Monte-Carlo realizations. The swapping criterion of W18 has been applied, i.e., a pair of planets is plotted only if the planets would still be detectable if their positions were swapped.

Finally, small planets can be detected in a fraction f of the stars while large planets can be detected in all the stars. With these assumptions, the intrinsic ratio of the number of small planets to the number of large planets is $r = p_1/p_2$.

We now compile a catalog of planets from this population. There are Np_1 small planets of which a fraction f are detectable, so the catalog will contain $N_1 = Np_1f$ small planets. There are Np_2 large planets, which are all detectable, so the catalog contains $N_2 = Np_2$ large planets; of these, $N_2' = Np_2f$ are in systems where a small planet could be detected. The complete catalog contains $N_{\rm cat} = N_1 + N_2 = N(p_1f + p_2)$ planets or stars. The fraction of these in which a small planet could be detected is $(N_1 + N_2')/N_{\rm cat}$ which we set equal to an inverse weight, w^{-1}. Then according to the balanced bootstrap procedure based on equation (4), we estimate that the ratio of the number of small planets to the number of large planets is

$$r_{\rm est} = \frac{N_1 w}{N_2} = r\frac{p_1 f + p_2}{p_1 + p_2}, \tag{5}$$

which is less than the true ratio r unless $f = 1$.

In the CKSM sample we have 909 planets, out of which 59 are large enough to be detectable at every position – these are the "large" planets in our example. The remaining 850 are "small" planets. This implies that in our example $p_2 \ll p_1$ or $r \gg 1$ and thus in doing a bootstrap analysis similar to the one in this Section one would arrive at the false conclusion that the intrinsic ratio of small to large planets is $r_{\rm est} \simeq rf + 1$—the limit of equation (5) if $r \to \infty$ while rf remains constant (if no detectability weighting is used at all $r_{\rm est} = rf$). Thus the balanced bootstrap simulations underestimate the occurrence rate of small planets by the fraction of positions in which they are detectable, which can be smaller than unity by a few orders of magnitude.

An important feature to note about the CKSM catalog is that it contains only systems with detected planets. One might ask whether the balanced bootstrap procedure of equation (4) would work if applied to a larger catalog, compiled with uniform selection criteria, in which only *some* of the systems had detected planets, i.e., the catalog before the stars with no detected planets are removed. This is the approach used for example by Petigura et al. (2013) and Fulton et al. (2017). However this procedure only works under special conditions, a key one of which is universality of all observed planetary systems and planet formation properties therein, see the Appendix.

5. ON THE DISTRIBUTION OF PLANETARY RADII

In our mock universe we set the intrinsic distribution of radii to a power law (eq. 1) with exponent $\gamma = 4$. Larger values of γ lead to a tighter correlation between $(R_p)_j$ and $(R_p)_{j+1}$, but produce fewer large planets ($R_p \gtrsim 4R_\oplus$), see Figures 3 and 4. We chose the simple integer exponent $\gamma = 4$ because it produces a correlation between the radii of the adjacent planets that is close to the observed Spearman $r_{\rm S} = 0.57$, a sizable population of large planets, and a scatter plot of $(R_{pj}, R_{p,j+1})$ points similar to the one observed in the CKSM catalog.

Other authors have carried out much more careful modeling of the planetary radius distribution. Burke et al. (2015) fit the distribution of radii between $0.7R_\oplus$ and $2.5R_\oplus$ to single and broken power laws. For single power laws they find $\gamma = 1.5$ with an allowed range from -0.5 to 3.25, although models with broken power laws are preferred. Petigura et al. (2013) find that the distribution is nearly flat in logarithmic radius (i.e., $\gamma = -1$) at the smallest radial range detected (1–$2R_\oplus$). A more recent study by Fulton et al. (2017), which employs the CKS data on single-planet systems, only considers planets with $R_p > 1.14R_\oplus$ and finds a significant gap in the radius distribution between $1.3R_\oplus$ and $2.4R_\oplus$. Millholland et al. (2017) fit the distribution to a broken power law with $\gamma = -0.5 \pm 0.2$ for radii less than $3R_\oplus$. Hsu et al. (2019) estimate the radius distribution between $0.5R_\oplus$ and $R_\oplus$ and their results can be fit approximately by $\gamma \approx 1$. Our distribution is steeper than any of these, but it is also important to point out that for the planets with $R_p \lesssim R_\oplus$ our knowledge of the occurrence rate is quite limited. Despite these limitations, our toy model produces a distribution of observed planets that is similar to the distribution in the real CKSM catalog (compare panels b and d in Figure 1). This toy model is a sufficient tool to illustrate the failure of the W18 bootstrap in de-biasing the observed radius distribution.

An obvious flaw of the simple power-law model is overproduction of small planets, which in turn implies the inability to recover the SNR distribution: in the CKSM data the fraction of planets with SNR$>$ 20 is 74%, while in our mock universe on average only about 35% of the planets have SNR$>$ 20 (see Figures 3 and 4). We address this issue in Section 7.

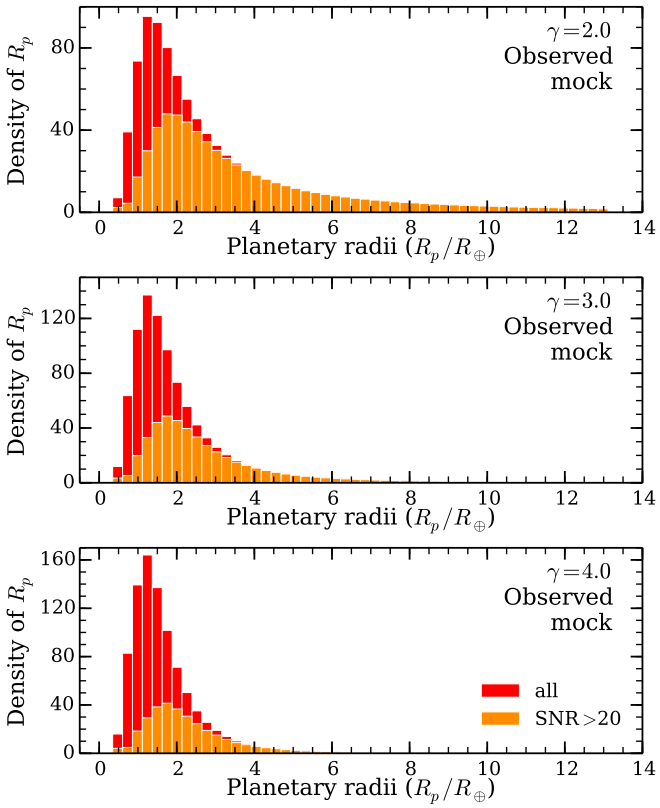


Figure 3. The mock observed planetary radii distribution (red) as a function of the exponent γ of the power-law distribution (eq. 1). The distributions of the planets with SNR> 20 are shown in orange. The plots each show an average of 5000 Monte-Carlo realizations. For the corresponding distributions in the CKSM catalog see Figure 7c.

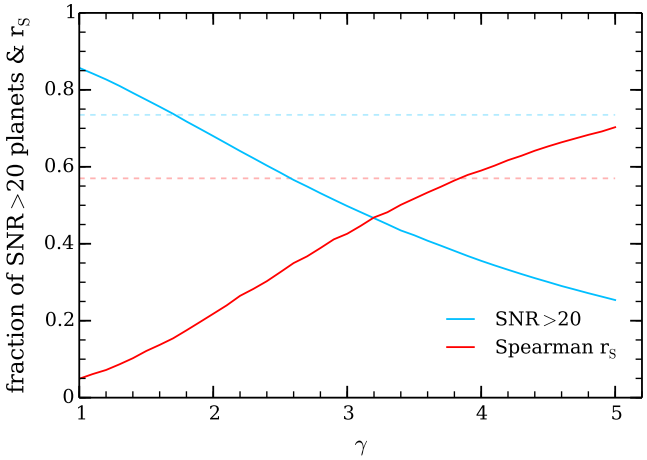


Figure 4. The value of the Spearman correlation coefficient r_S between the radii of adjacent planets (red) and the fraction of the planets with SNR> 20 in the mock observed planets (blue) as a function of he exponent γ of the power-law distribution (eq. 1). The faint dashed lines of the corresponding colors represent the observed values from the CKSM catalog.

6. CORRELATIONS OF RADII OF LARGE PLANETS

W18 comment that there are many pairs of large planets with both radii close to $8R_\oplus$, and that this correlation cannot arise from observational selection effects because all planets with these large radii are detectable. But is the correlation between the radii of adjacent planets significant for large radii? To quantify this, we have cut off the observed distributions in both the mock universe and the CKSM sample at a minimum radius $R_{\rm cut}$ and plotted the

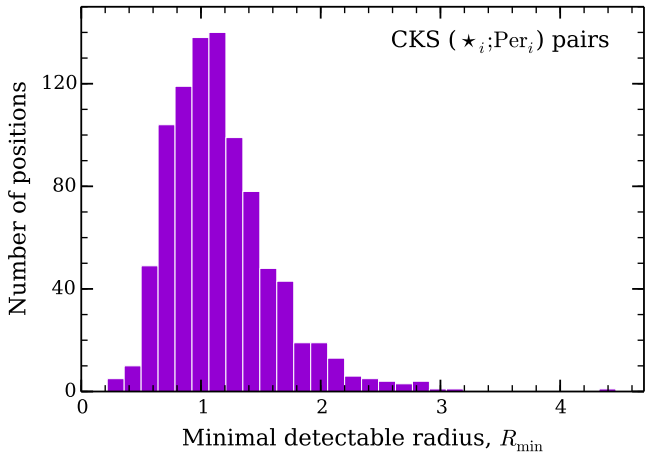


Figure 5. Smallest detectable radii. The number of available positions $(\star_i, \mathrm{Per}_i)$ as a function of the minimal detectable radius according to equation (2).

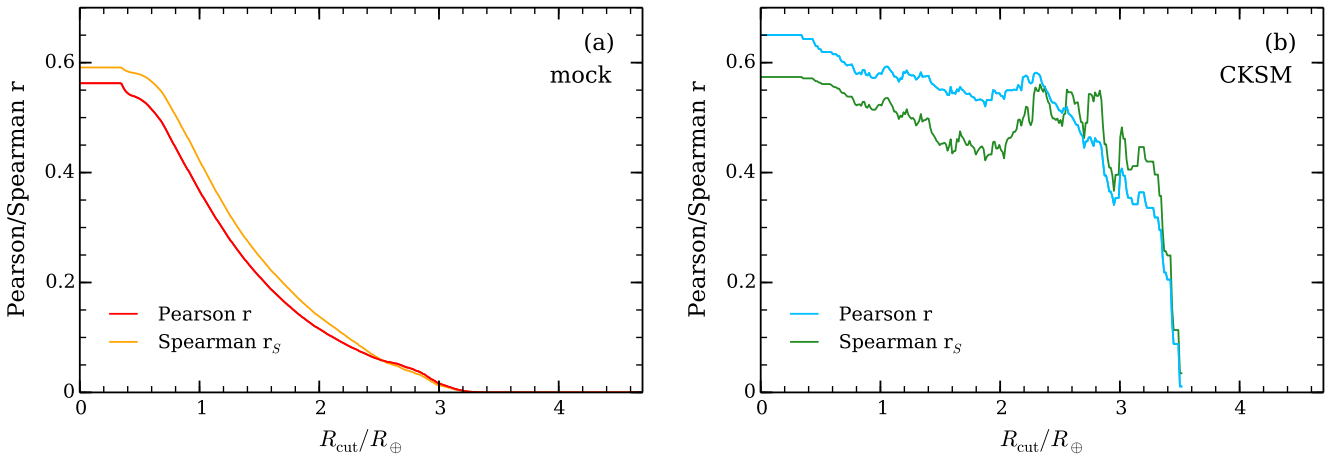


Figure 6. Pearson and Spearman correlation coefficients as a function of the minimum radius $R_{\rm cut}$ of planets included in the correlation, i.e., $R_{pj}, R_{p,j+1} \geq R_{\rm cut}$. (a) Pearson r (red) and Spearman r_s (yellow) for the mock universe. We plot the average of 25,000 Monte-Carlo realizations. The median Pearson/Spearman p-value is < 0.01 for $R_{\rm cut} \leq 1.47/1.56 R_\oplus$ and rises to > 0.4 by $R_{\rm cut} \simeq 2.2 R_\oplus$. (b) Pearson r (blue) and Spearman r_s (green) for CKSM data. The Pearson/Spearman $p < 0.03/0.01$ at $R_{\rm cut} \leq 3.3 R_\oplus$, showing that the correlation is significant at a level of a few percent or better, but rises steeply to $> 0.5/0.6$ at $R_{\rm cut} = 3.45 R_\oplus$.

correlation coefficients as a function of $R_{\rm cut}$ in Figure 6. We see that no significant correlation between the radii of adjacent planets with $R_p > 3.4 R_\oplus$ is present in the CKSM data.

Nevertheless there are differences between the power-law toy model and the data. In particular, the correlation between R_{pj} and $R_{p,j+1}$ in the CKSM sample persists up to a cutoff radius $R_{\rm cut} \simeq 3.4 R_\oplus$, whereas the correlation declines in the mock catalogs for $R_{\rm cut} \gtrsim 1 R_\oplus$ and becomes weak by about $1.5 R_\oplus$ (see left panel of Figure 6). This is not surprising as the correlation in the mock universe is due to observational biases, which are dominated by the distribution of smallest detectable radii (Figure 5). This distribution is rapidly falling for $R_p \gtrsim 1.2 R_\oplus$. If the width of the distribution of the minimal detectable radii were larger, the correlation should persist to larger radii.

We conclude that the extremely simple model of hypothesis (i)—"planets don't know anything"—can successfully reproduce the overall correlation between adjacent planet radii seen in W18 (Figure 1). In this sense it provides a counter-example to W18's arguments that the observed correlation must be astrophysical. However, other data indicate that hypothesis (i) cannot be the whole explanation: the SNR distribution is not consistent with the data, the correlation is weaker than observed for radii between $R_\oplus$ and $3 R_\oplus$, and the radius distribution is too steep. We therefore turn to hypothesis (ii).

7. "PLANETS KNOW ABOUT THE SYSTEM THEY FORMED IN". REPRODUCING THE SNR DISTRIBUTION.

In this Section we complicate the rules guarding our mock universe. We assume that "planets know about the system they formed in", that is, that the distribution of planetary radii may vary from system to system. This is a very plausible hypothesis, since the distribution of radii presumably depends on the properties of the protoplanetary disk which differ for every star. We demonstrate that with this assumption we can reproduce the distribution of planetary radii observed in the CKSM catalog, the distribution of SNR, and even the correlation coefficients between the radii of adjacent planets.

We consider four types of planetary systems (α_a, α_b, α_c, α_d):

(a) Systems with predominantly small planets. For these systems, similarly to Section 2, we set the planet radius distribution to a power-law $p(R_p|\alpha_a) \sim R_p^{-\gamma}$;

(b) Systems in which planets tend to have $R_p \simeq 1.3R_\oplus$. We model the radius distribution as a log Gaussian,

$$p(R_p|\alpha_b) \sim \exp\left[-\frac{(\log(R_p) - \log(R_1))^2}{2\sigma_1^2}\right]; \tag{6}$$

(c) Systems in which planets tend to have $R_p \simeq 2.4R_\oplus$. We again model the radius distribution with a log Gaussian,

$$p(R_p|\alpha_c) \sim \exp\left[-\frac{(\log(R_p) - \log(R_2))^2}{2\sigma_2^2}\right]; \tag{7}$$

(d) Systems with large planets. Here $p(R_p|\alpha_d) \sim R_p^{-1}$ for $R_p \geq R_d$ and $p(R_p|\alpha_d) = 0$ for $R_p < R_d$. All such large planets are detectable and thus one may expect that their observed distribution is close to their intrinsic distribution.

To generate a set of mock CKSM planetary systems, we randomly assigned CKSM systems to one of the above distributions with probability P_μ, where $\mu = a, b, c, d$ and $\sum_\mu \mathrm{P}_\mu = 1$, using a similar procedure to the one discussed in Section 2[5]. For each set of nine parameters γ, R_1, σ_1, R_2, σ_2, R_d, P_b, P_c and P_d we generate 100 mock systems and average their parameters. We evaluate the quality of the fit between the mock systems and the CKSM catalog based on the following criteria: (1) Maximizing the p-value of the Kolmogorov–Smirnov (KS) comparison test between the mock and true observed planetary radius distributions; (2) Maximizing the p-value of the KS comparison between the mock and true observed planetary radius distributions detected with SNR>20; (3) the Spearman correlation coefficient r_p of the correlations between adjacent planetary radii must be close to the observed value; (4) The fraction of $R_{p,j+1}(R_{p,j})$ pairs that fall into the boxes $(R_{p,j+1}, R_{p,j}) < 1R_\oplus$, $1R_\oplus < (R_{p,j+1}, R_{p,j}) < 2R_\oplus$, $2R_\oplus < (R_{p,j+1}, R_{p,j}) < 4R_\oplus$, and $(R_{p,j+1}, R_{p,j}) > 4R_\oplus$ must be close to the values observed in the CKSM catalog[6].

Figure 7 presents an example Monte-Carlo realization of the four-component universe side-to-side with the CKSM data. The parameters used to generate this realization are

$$\begin{gathered}\gamma = 3.2, \quad R_1 = 1.42R_\oplus, \quad \sigma_1 = 0.12, \quad R_2 = 2.35R_\oplus, \quad \sigma_2 = 0.23, \quad R_d = 3.4R_\oplus \\ \mathrm{P}_a = 1 - \mathrm{P}_b - \mathrm{P}_c - \mathrm{P}_d, \quad \mathrm{P}_b + \mathrm{P}_c = 0.54, \quad \mathrm{P}_b/(\mathrm{P}_b + \mathrm{P}_c) = 0.3, \quad \mathrm{P}_d = 0.035.\end{gathered} \tag{8}$$

We did not explore the parameter space too deeply, as the purpose of this work is to demonstrate that the correlations observed by W18 may be explained by hypothesis (i) or (ii) of the Introduction without resort to hypothesis (iii). There likely exists a set of parameters and a set of modifications to the assumed distributions $p(R_p|\alpha_\mu)$ above that do an even better job of reproducing the CKSM data. Despite this limited search, the parameters (8) provide an excellent fit to the overall distribution of radii in the CKSM data. In particular, the mock planetary radius distributions for all the observed planets and for those with SNR>20 as well as the correlations between the radii of adjacent planets are nearly identical to the data. On average we find $64 \pm 2\%$ of planets with SNR>20 in agreement with $\sim 70\%$ in

[5] In the case of a randomly assigned distribution failing to deliver detectable planets in a given system, which we defined as 10,000 failed attempts, we reassigned the system to another mock distribution. The reassignments are rare, happening on average for 1% of the systems.

[6] For consistency of the comparison tests we removed the system K03158. All five planets in the system were obvious outliers in the SNR(R_p) distribution.

the CKSM data; the probability that the radius distributions for all observed planets and those with SNR> 20 are identical to the respective CKSM distributions is $40 \pm 30\%$; and the average Spearman correlation coefficient between the radii of adjacent planets $r_S = 0.57 \pm 0.04$ is also in complete agreement with the observed value of 0.56. In the four-component mock universe the correlation between the radii of the adjacent planets persists until $R_p \simeq 3.3R_\oplus$ (Figure 8), which is also in agreement with the CKSM data presented on Figure 6b. The average fraction of points on the $R_{p,j+1}$ vs. $R_{p,j}$ plot (with the W18 swapping criterion applied) falling into the box $(R_{p,j+1}, R_{p,j}) < 1R_\oplus$ is 0.02 ± 0.01, the box $1R_\oplus < (R_{p,j+1}, R_{p,j}) < 2R_\oplus$ is 0.26 ± 0.2, the box $2R_\oplus < (R_{p,j+1}, R_{p,j}) < 4R_\oplus$ is 0.35 ± 0.3, and the box $(R_{p,j+1}, R_{p,j}) > 4R_\oplus$ is 0.04 ± 0.1 in good agreement with 0.04, 0.021, 0.29, and 0.04, respectively, for the CKSM data.

It is indeed easy to produce an "observed mock" distribution of planetary radii that is similar to the one observed in CKSM (see Figure 7ac) using the nine free parameters describing the systems α_a, α_b, α_c and α_d. What is not easy or obvious is that we can reproduce all the following characteristics together – the distribution of planetary radii, the distribution of planetary radii with SNR> 20, the correlation between the radii of adjacent planets, the visual appearance of such a distribution, and the Pearson and Spearman correlation coefficients as a function of the minimum radius $R_{\rm cut}$ of planets included in the correlation. The last of these characteristics is the hardest to reproduce. One may naively think that mere presence of the α_b and α_c systems, which predominantly have planets in the vicinity of R_b and R_c, would give us a correlation between the radii of adjacent planets up to $R_{\rm cut} \simeq R_b$. This however is not the case. Such a correlation extends only to $R_{\rm cut} \simeq R_a \simeq 1.4R_\oplus$. The small-planet systems α_a have the intrinsic density $\sim R_p^{-3.2}$, which produces a considerably weaker correlation at smaller radii than the one observed in CKSM. The large-planet systems α_d have the intrinsic density $\sim R_p^{-1}$, which produces no significant correlation between the radii of adjacent plants at all. It is nontrivial that the combination of α_a, α_b, α_c and α_d produces the entire suite of observations described at the start of this paragraph and shown in Figures 7 and 8.

Note that sampling from the combined four-component distribution in the same way as we sampled in Section 3 and 4 when considering hypothesis (i) would not produce as strong a correlation between the radii of adjacent planets as on Figure 7bd. The results would look similar to Figures 2adcf.

In summary, we have demonstrated that a correlation between the radii of adjacent planets that is statistically indistinguishable from the correlation found by W18 can arise simply from assuming that planets are formed in systems of several distinct types.

8. SUMMARY

We have shown that the apparent correlation between the radii of adjacent planets found by Weiss et al. (2018) can arise in two simple toy models, neither or which requires that planets "know about" the properties of their neighbors.

The first toy model correctly reproduces the correlation, although at the cost of an SNR distribution that is not consistent with the data and a radius distribution that is steeper than observed. Nevertheless, it shows that the correlation can arise in part from observational selection effects: in host systems that are difficult to observe—because of large stellar radii, photometric noise, or other system properties—all detected planets will have large radii, while in systems that are easy to observe most planets will have small radii close to the detection limit. This conclusion is similar to the argument of Zhu (2019), although based on quite different methods. This hypothesis assumes that the planets "don't know anything"; that is, that their probability of formation is guided by a universal distribution function that depends only on the planetary radii.

Our second toy model does not suffer from this shortcoming. This model is based on the hypothesis that planets "know about the system they formed in", that is, that the distribution of planetary radii may vary from system to system. With a simple version of this hypothesis requiring only four types of system we can reproduce the distribution of planetary radii observed in the CKSM catalog, the distribution of SNR, and even the correlation coefficients between the radii of adjacent planets.

We have also shown that the bootstrap simulations used by Weiss et al. (2018), as well as an improved simulation that weights planets by their detectability, are statistically biased in that they seriously underestimate the occurrence rate of small planets, and therefore generate radius distributions that are less steep than the true distribution. Therefore this method cannot be used either to derive the planetary radius distribution or to argue for the astrophysical nature of the correlation of the radii of adjacent planets.

W18 also found correlations in other properties of the planets in multi-planet systems, but we have not analyzed these findings.

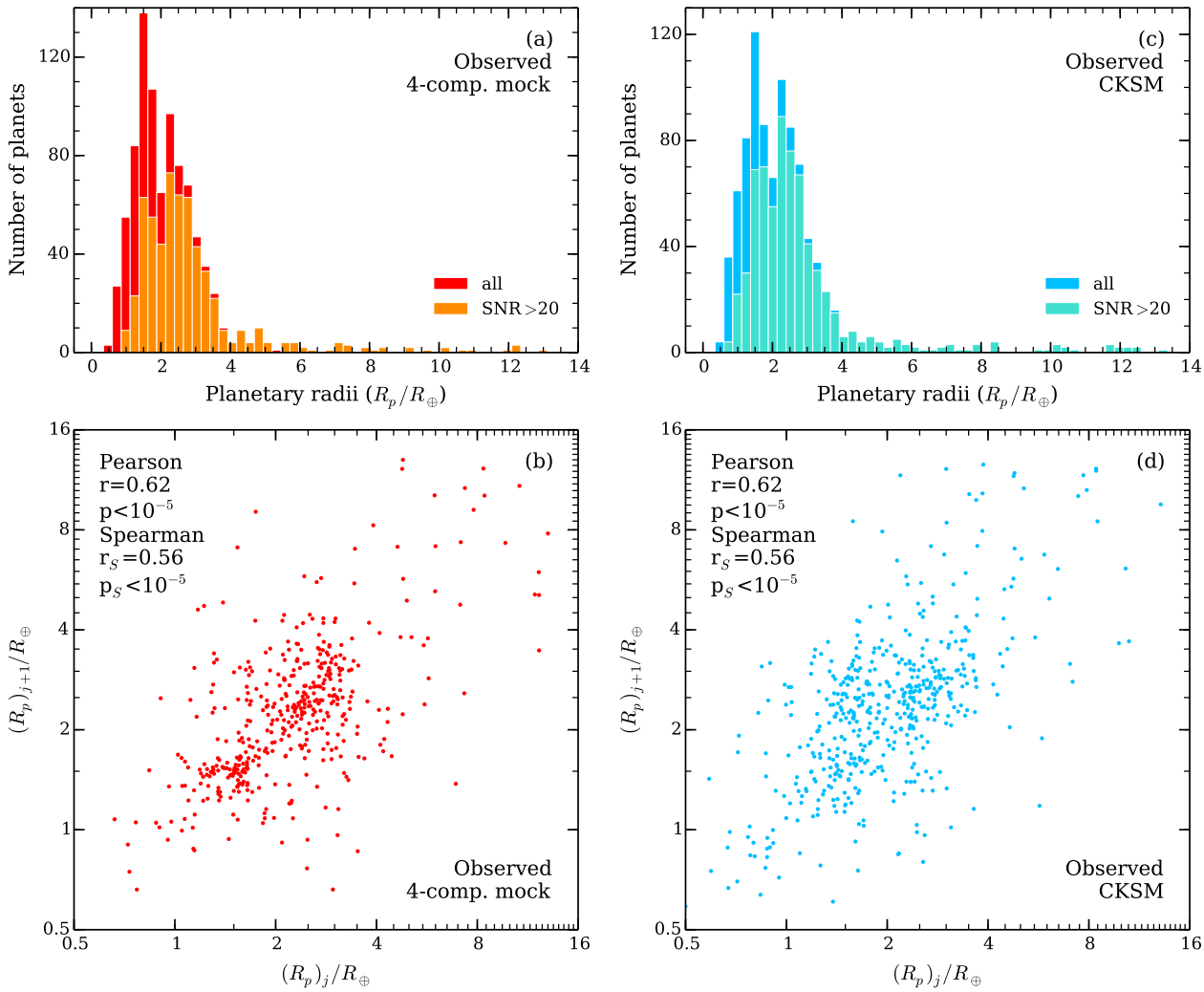


Figure 7. Observations in the four-component mock universe compared to the CKSM sample. Red/orange plots belong to an example Monte-Carlo realization in the mock universe and blue/green to the observed planets. (a) The distribution of radii of the observed mock planets. We randomly assign each of the 354 CKSM systems (see footnote 7) to one of the four distributions described in Section 7 and for each available $(\star_i, \mathrm{Per}_j)$ position in the system, we draw a radius at random from the assigned mock distribution, apply the SNR cut of equation (2), and repeat until the planet survives the cut. (b) The relation between the radii of adjacent planets R_{pj} and $R_{p,j+1}$ for the Monte-Carlo realization of mock planets plotted in (a). (c) and (d) The distribution of radii and the relation between the radii of adjacent planets in the CKSM sample. Concerning the difference with Figure 1e refer to footnote 7. In panels (b) and (d) we applied the swapping criterion of W18, i.e., a pair of adjacent planets is plotted only if the planets would still be detectable if their positions were swapped.

The solution to the bias problems that have plagued these analyses is to perform Bayesian analyses of the entire Kepler catalog, rather than just stars that have detected planets, and to include detailed models for the planet detection and vetting probability.

Millholland et al. (2017) have found similar correlations in the distribution of masses in a much smaller sample of *Kepler* multi-planet systems (37 systems and 89 planets). They concentrated on the correlation with respect to planetary masses, using masses derived from transit timing variations. In their tests they use a bootstrap algorithm that re-samples from the observed distribution, and thus is subject to the same criticisms as the bootstrap used in Weiss et al. (2018); however, the main selection effects in their catalog arise from mutual inclinations and period ratios so the bias introduced by this method may be small.

ACKNOWLEDGEMENTS

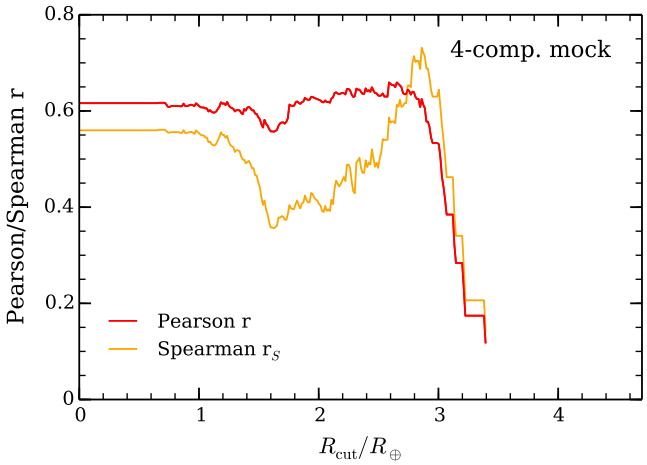


Figure 8. Pearson and Spearman correlation coefficients as a function of the minimum radius $R_{\rm cut}$ of planets included in the correlation, i.e., $R_{pj}, R_{p,j+1} \geq R_{\rm cut}$, for the four-component Monte-Carlo realization in Figure 7ab. The Pearson/Spearman $p < 0.02/0.01$ at $R_{\rm cut} \leq 3.1R_\oplus$, showing that the correlation is significant at a level of a few percent or better, but rises steeply to ~ 0.3 at $R_{\rm cut} = 3.2R_\oplus$ and to ~ 0.5 at $R_{\rm cut} = 3.4R_\oplus$. Compare Figure 6.

We are grateful to Kento Masuda, Erik Petigura, Lauren Weiss, Wei Zhu, and the anonymous referees for perceptive and useful comments. LM's support at the IAS is provided by the Friends of the Institute for Advanced Study.

REFERENCES

Burke, C. J., Christiansen, J. L., Mullally, F., et al. 2015, ApJ, 809, 8, doi: 10.1088/0004-637X/809/1/8

Christiansen, J. L., Jenkins, J. M., Caldwell, D. A., et al. 2012, PASP, 124, 1279, doi: 10.1086/668847

Fulton, B. J., Petigura, E. A., Howard, A. W., et al. 2017, AJ, 154, 109, doi: 10.3847/1538-3881/aa80eb

Gilbert, G. J., & Fabrycky, D. C. 2020, arXiv e-prints, arXiv:2003.11098. https://arxiv.org/abs/2003.11098

He, M. Y., Ford, E. B., & Ragozzine, D. 2019, MNRAS, 490, 4575, doi: 10.1093/mnras/stz2869

Hsu, D. C., Ford, E. B., Ragozzine, D., & Ashby, K. 2019, AJ, 158, 109, doi: 10.3847/1538-3881/ab31ab

Kipping, D. 2018, MNRAS, 473, 784, doi: 10.1093/mnras/stx2383

Millholland, S., Wang, S., & Laughlin, G. 2017, ApJL, 849, L33, doi: 10.3847/2041-8213/aa9714

Mulders, G. D., Pascucci, I., Apai, D., & Ciesla, F. J. 2018, AJ, 156, 24, doi: 10.3847/1538-3881/aac5ea

Petigura, E. A., Howard, A. W., & Marcy, G. W. 2013, Proceedings of the National Academy of Science, 110, 19273, doi: 10.1073/pnas.1319909110

Pu, B., & Wu, Y. 2015, ApJ, 807, 44, doi: 10.1088/0004-637X/807/1/44

Sandford, E., Kipping, D., & Collins, M. 2019, MNRAS, 489, 3162, doi: 10.1093/mnras/stz2350

Weiss, L. M., & Petigura, E. A. 2019, arXiv e-prints, arXiv:1908.05833. https://arxiv.org/abs/1908.05833

Weiss, L. M., Marcy, G. W., Petigura, E. A., et al. 2018, AJ, 155, 48, doi: 10.3847/1538-3881/aa9ff6

Zhu, W. 2019, arXiv e-prints, arXiv:1907.02074. https://arxiv.org/abs/1907.02074

APPENDIX

A. BALANCED BOOTSTRAP SIMULATIONS IN A CATALOG CONTAINING SYSTEMS OF DIFFERENT TYPES

Let us assume we have a catalog containing N stars that may or may not have detectable planetary systems. A fraction k_α of them belong to a type α and the rest k_β to a type β ($k_\alpha + k_\beta = 1$). There are two types of planets, having radii R_1 and $R_2 > R_1$. Systems α have small R_1 planets with probability p_1 and large R_2 ones with probability p_2. Systems β have large R_2 planets with probability q_2 and small ones with probability q_1. Large planets R_2 are always detectable. Small planets are detectable with probability f_α in the α-systems and probability f_β in the β-systems.

In the universe we have $Nk_\alpha p_1 + Nk_\beta q_1$ small planets and $Nk_\beta q_2 + Nk_\alpha p_2$ large planets. In the catalog we have $Nk_\alpha p_1 f_\alpha + Nk_\beta q_1 f_\beta$ small planets and $Nk_\alpha p_2 + Nk_\beta q_2$ large planets. The intrinsic ratio of small planets to large ones is

$$r = \frac{k_\alpha p_1 + k_\beta q_1}{k_\alpha p_2 + k_\beta q_2}. \tag{A1}$$

Small planets would be detectable in $Nk_\alpha f_\alpha + Nk_\beta f_\beta$ of systems. Now let us try to reconstruct the intrinsic ratio of small planets to large one using the weighting

$$r_{\rm est} = \frac{\text{(number of small planets in the catalog)}}{\text{(number of large planets in the catalog)}} \times \frac{\text{(total number of systems observed)}}{\text{(number of systems in which small planets could be detected)}}.$$

We have

$$r_{\rm est} = \frac{Nk_\alpha p_1 f_\alpha + Nk_\beta q_1 f_\beta}{Nk_\beta q_2 + Nk_\alpha p_2} \frac{N}{Nk_\alpha f_\alpha + Nk_\beta f_\beta} = r \frac{k_\alpha p_1 f_\alpha + k_\beta q_1 f_\beta}{k_\alpha p_1 + k_\beta q_1} \frac{1}{k_\alpha f_\alpha + k_\beta f_\beta}. \tag{A2}$$

The estimated ratio coincides with the true one only if $f_\alpha = f_\beta$ or $p_1 = q_1$. Otherwise there is no way to reconstruct the intrinsic occurrence unless we know which systems are type α and which are β. However it may not always be possible to distinguish systems α from systems β using observations of the current properties of the systems. There may be properties of the protoplanetary disk that were erased when the planets were formed and the star blew away the remainder of the disk.